FEDERAL UNIVERSITY OF TECHNOLOGY, AKURE
JOURNAL OF ENGINEERING AND ENGINEERING TECHNOLOGY

DEVELOPMENT OF A PULVERIZING MACHINE FOR RAPHIA PALM SEEDS

[1]Akinola, A. O., [2]Olusola, E. O. and [1]Olundegun, S. A.

[1]Department of Mechanical Engineering, Federal University of Technology Akure, Ondo State, Nigeria
[2] Olusegun Agagu University of Science and Technology, Okitipupa, Nigeria

**Correspondence: akinteche@yahoo.com*

Akinola, A. O., Olusola, E. O., and Olundegun, S. A. (2025): Development of a Pulverizing Machine for Raphia Palm Seeds. *FUTA Journal of Engineering and Engineering Technology* /19(1), 52-65

Received Date: 15.08.24 **Accepted Date: 15.10.24**

Abstract
The growing concern about transitioning energy generation from fossil fuels to alternative renewable energy resources in order to help satisfy the world's energy needs and sustainable environment has made researchers explore various alternative energy options. Biomass remains a distinctive choice among the alternatives possible. This research is aimed at developing a machine for pulverizing Raphia seed. The approach to this research involves the design of components of the machine; Finite element analysis (FEA) analysis of the structural parts of the designed machine; fabrication and assembling of components and design of experiment for evaluating the performance of the machine. FEA analysis of the 3D CAD model for rotor and frame assembly was done using Autodesk Inventor. The result showed that the maximum stress of 103.1 MPa and 97.74 MPa respectively experienced by the members of the rotor and frame assembly are within safe values, and is not susceptible to structural failure during operation. Performance evaluation revealed the machine has a throughput of 11.85 kg/hr., a pulverizing efficiency of 97% and can pulverize to an average particle size of 624 µm.

Keywords: *Raphia seeds, pulverizing, throughput, efficiency, structural failure*

Introduction

Energy is an indispensable need for humanity and also the driving force for the development of every nation. The increasing energy consumption; depleting and increasing prices of fossil resources; and the adverse environmental impact of greenhouse gas emission are key factors to the global energy challenge, which has put the world on a quest for new alternatives to secure the future energy demand (BP, 2017; EIA, 2016; Lund and Salgi, 2009). According to Atadashi et al. (2011) and Oshewolo (2012), non-renewable energy sources contribute over 86% of the global energy supply and are depleting rapidly. These problems have thus intensified the global search for alternative energy means and sustainable technology that can counter the shortcomings of non-renewable energy sources (Fapetu et al., 2018).

Over the last decade, there has been a rise of a number of alternative energy sources. While the viability of each can be argued, they all contribute something positive when compared to fossil fuels. Lower emissions, lower fuel prices and the reduction of pollution are all advantages that the use of alternative fuels can often provide (Owusu and Asumadu-Sarkodie, 2016). Biomass seems to be more promising as a source of renewable energy as it is more reliable and sustainable. Biomass energy is obtained either by direct burning or by converting biomass to a more conventional form of solid fuels such as briquette, dung, cakes or in a pulverized form; or into liquid fuels such as ethanol and bio-diesel; or into gaseous fuels (biogas) (Garg et al., 2007; Ramages and Scurlock, 1996).

Raphia palm tree is one of the most economically useful plants in Africa. Every part of the tree has many uses. The leaves are used as material for furniture and shelter construction; sap from the trunk is fermented into palm wine; and the fruit is used to produce edible oil (Dauda et al., 2018; Akpan and Usoh, 2004). According to Dauda et al. (2018), there are about five species of it in Nigeria and they are found dominantly in the southern part of the country. Raphia palm fruits and seeds are shown in Plates 1 and 2 respectively.

Raphia palm seeds are very hard. Dauda et al. (2018) reported a breaking force of 30.06 kN at 9.6% moisture level. Pulverizing the seed can accomplished through the process of crushing and grinding. Due to this high hardness, there is need to develop an efficient machine for pulverizing the seed into fine uniform form. Dauda et al. (2018) conducted a study to determine the physical and

Plate 1: Raphia palm fruits

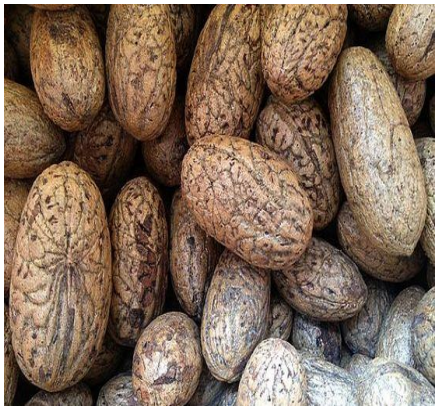

Plate 2: Raphia palm seeds

mechanical properties of Raphia palm kernel at three different moisture content levels of 9.69%, 14.69%, and 19.69%. The result of the physical properties of the kernel determined revealed that the major diameter, intermediate diameter, minor diameter, geometric mean diameter, sphericity, surface area, true density, bulk density, porosity, and angle of repose respectively ranged between, 42.41-43.43 mm, 35.88-36.69 mm, 23.81-25.31 mm, 33.09-34.29 mm, 7.80-7.93, 32.01-34.31 cm2, 1.17-1.50 g/mm3, 0.8-1.19 g/mm^3, 31.62-42.18%, 40.24-42.18o and coefficient of static friction ranged between 2.55-0.44 and 0.5-0.14 on plywood and steel respectively. While the mechanical properties ranged between 11.01-30.06 kN for maximum force, 5.6-12 kN for bio-yield point and 10.55-12.75 mm for deformation on horizontal loading and 9.44-11.77 kN for maximum force, 4.7-3.8 kN for bio-yield point and 8.1-7.70 mm deformation on vertical loading. A conclusion drawn from the study is that at higher moisture content, the sample breaks faster as moisture content was observed to have an influence on the compressive strength of Raphia palm kernel. Similarly, Fabunmi et al. (2015) investigated the physical and mechanical properties of Raphia seed. The geometric mean diameter and sphericity are 32.85 mm and 50.74 %, respectively. The peak values of force and deformation at break were 12.925 kN and 14.050 mm, respectively. It was observed that the pressure in cracking the seed in longitudinal position is greater than when placed in transverse or natural position. Both studies provide data for efficient handling and equipment design. However, they both did not investigate the combustion process and characteristics of Raphia seed. Muhammed (2013) developed a rough grinding equipment to grind biomass materials and produce standard size of particle materials. In the research, finite element analysis technique was used to predict the displacement magnitude and identify the worst stress locates in the structures using SolidWorks Simulation. Egbe and Olugboji (2016) developed a double roll crusher from locally available materials for low hardness rocks. The throughput capacity of the machine was 1.43tonnes/hour. The theoretical efficiency of the double roll crusher when crushing limestone was 60% while that of kaolin was 80%. Kawuyo et al. (2017) conducted a study to carry out the performance evaluation of a grain milling machine using maize (Sammaz - 12 variety) and millet (Lake Chad Dwarf variety) at different moisture range of 8.3% to 24.6% and 6.4% to 27.2% (db) respectively. this machine works by impact action of the rotary hammers. The rotating hammers are directly driven by the petrol engine outlet shaft. As grains are delivered into the milling chamber from the hopper, they are hit by the rotating bars against the flat bars fixed around the drum. It was found that, the milling efficiency and milling rate decreased from 86.3% to 40% and 20.4 to 12.5kg/h for maize respectively and 89% to 26.6% and 23.4 kg/h to 12.1 kg/h for millet respectively as the moisture content was increased. Ngabea et al. (2015) developed a magnetic sieve grinding machine that was used to grinds corn, cassava, millet, guinea corn to flour. The machine is powered by a 5.96 kW diesel engine. Performance evaluation showed that 10.5 g of the machine parts were worn out after 10 hours of grinding. The throughput capacity and the efficiency of the machine are 600 kg/hr and 87.5% respectively. Ugwuegbu et al. (2017) developed a 5 kg laboratory ball mill which was tested using limestone as feed material. Bond's equation was used to calculate the specific and shaft powers required to drive the mill at the specified capacity, and also to size the mill. The design results show that the minimum shaft power required to drive the ball mill is 0.2025 horsepower, the length of the mill at a fixed mill diameter of 210 mm is 373 mm, and the required shaft length and diameter are 712.2 mm and 30 mm respectively. The results of the particle size analysis, before and after the grinding test, show that the values of F50, F80, P50, and P80 of the limestone that was fed into the mill are 650 microns, 1950 microns, 47.5 microns and 85 microns respectively.

The works available in literature provides a good background information and designed procedures for the development of pulverizing machine. However, there is need to develop a machine that can be used to pulverize Raffia seed, having its unique mechanical properties of high breaking force, into standard particle sizes. Therefore, this work aimed at developing a pulverizing machine for Raffia seeds.

Materials and Method

Materials and Equipment

The tools and equipment used for the work are meter rule and vernier caliper for taking the measurement; scriber for marking out; hacksaw for cutting operation; vice for holding the workpiece; welding machine for welding process, spanner and screwdriver for fastening parts with bolt and nut or screws as the case may be; and grinding machine for cutting and finishing off worked surfaces.

Method

Hopper design

The Raphia seed is fed into the machine through the hopper, with frustrum cross-section and dimensions as shown in Figure 1.

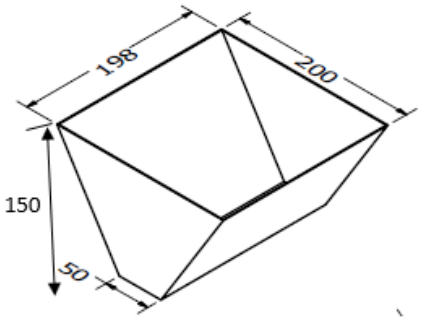

Figure 1: Hopper

The volume of the hopper is determined using Equation (1).

$$V_h = V_{fp} - V_{cp} \quad (1)$$

Where: V_h is the volume of hopper, V_{fp} is the volume of full pyramid, and V_{cp} is the volume of the pyramid section cutaway.

The volume of a regular pyramid is given by Equation (2).

$$V_{pyramid} = {}^1/_3 \; x \; b \; x \; h \quad (2)$$

where b is the base area and h is the height of the pyramid.

$$V_h = 0.00924 \text{ m}^3$$

Determination of shaft speed

The pulley of the rotating hammer shaft is designed to be bigger in order to trade speed for shaft power. The shaft speed is thus determined using Equation (3) (Khurmi and Gupta, 2010).

$$\frac{D_{emp}}{D_{emp}} = \frac{N_{emp}}{N_{emp}} \quad (3)$$

where:
D_{emp} is the diameter of the electric motor pulley (125 mm); D_{emp} is the diameter of the main shaft pulley (200 mm); N_{emp} is the speed of the electric motor (2500 rpm); and N_{emp} is the speed of the hammer shaft. N_{emp} = 1562.5 rpm.

Determination of the power required to crush the seed

The power required to crush the seeds is determined using Equation (4) (Kovács, and Kerényi, 2019; Shan et al., 2024).

$$P_c = T_c \; x \; \omega \quad (4)$$

where:
P_c is the power required by the hammer; T_c is the breaking or crushing torque; ω is the angular velocity of the shaft.

The breaking or crushing torque T_c is obtained using Equation (5) (Oji et al., 2019).

$$T_c = F_c \; x \; r \quad (5)$$

where:
F_c is the is the force required to break or crush the Raphia seed given in Dauda et al. (2018) to be 30.06 kN; r is the distance from the axis of the shaft and the head of the hammer (75 mm).

$$T_c = 2.2545 \text{ kNm}$$

The angular velocity of the shaft (ω) is obtained using Equation (6) (Khurmi and Gupta, 2010).

$$\omega = \frac{2\pi N_{msp}}{60} \quad (6)$$

ω = 163.6 rad/s

Therefore, the power required by the hammer Pc to crush the seed is obtained by substituting the determined parameters into Equation (4).

Pc = 268.8 kW

Power required on the main shaft

The power required on the main shaft is supplied by electric motor. It is obtained using Equation (7)

$$P_{m.s} = \text{Pc} \times SF \quad (7)$$

where:

$P_{m.s}$ is the power required on the main shaft; and SF is service factor 1.3

Using a service factor of 1.3, power required on the main shaft is thus obtained

$P_{m.s}$ =349.44 kW

Selection of belt type

Considering the power required on the main shaft (349.44 kW), standards (IS: 2494-1974) for belt drive was consulted to select belt type. Belt type E was selected with 125 mm and 200 mm driver and driven pulley diameters respectively (Khurmi and Gupta, 2010).

Determination of belt power transmission centre distance and length

The power required by the main shaft and hammer assembly is provided by the electric motor through belt power transmission system represented by the schematic diagram in Figure 2.

According to Udo et al. (2015), the maximum and the minimum centre distances can be obtained using Equations (8) and (9), and the average given by Equation 10.

$$C_{max.cd} = 3(D_{emp} + D_{emp}) \quad (8)$$

$$C_{min.cd} = 0.55(D_{emp} + D_{msp}) \quad (9)$$

$$C_{avg.cd} = \frac{C_{min.cd} + C_{max.cd}}{2} \quad (10)$$

where:

D_{emp} and D_{msp} is the diameter of the electric motor and main shaft pulleys, given to be 125 mm and 200 mm respectively;

$C_{min.cd}$ is the minimum centre distance (975 mm); $C_{max.cd}$ is the maximum centre distance (378.75 mm); $C_{avg.cd}$ is the average centre distance (677 mm).

Given that the selected centre distance (Ccd) must fulfil the following conditions:

$C_{min.cd} \leq \text{Ccd} \leq C_{max.cd}$; and $\text{Ccd} > D_{emp}$

therefore, a centre distance of 550 mm was selected and a correction factor of 0.95 corresponding to the centre distance is chosen.

The belt pitch length (L_{belt}) is which is the circumferential length at the pitch width is obtained according to Khurmi and Gupta (2008) using Equation (11)

$$L_{belt} = 2\text{Ccd} + 1.57\left(D_{emp} + D_{msp}\right) + \frac{(D_{emp} + D_{msp})^2}{4C_{cd}} \quad (11)$$

L_{belt} = 1612.8 mm

Design of main shaft rotor assembly

On the main shaft, a set of hammers separated by spacers held together by mounting rods are mounted to form as rotor assembly as shown in Figure 3.

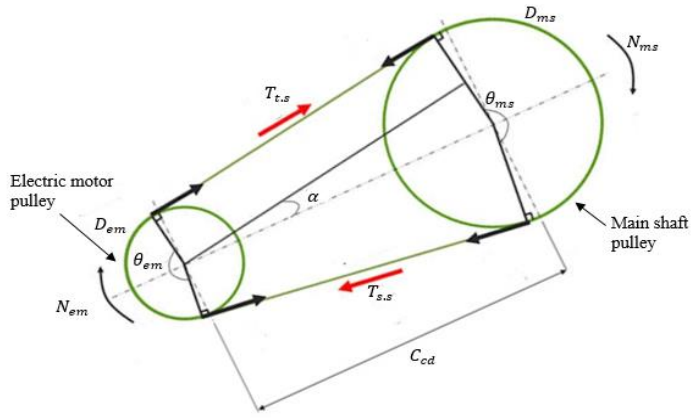

Figure 2: Schematic diagram of the power transmission from electric motor to main shaft

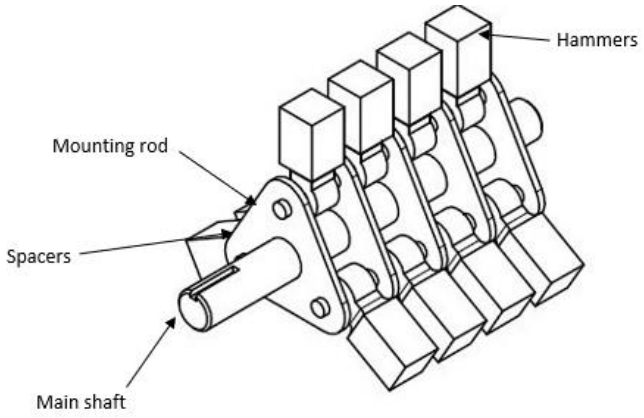

Figure 3: Rotor assembly

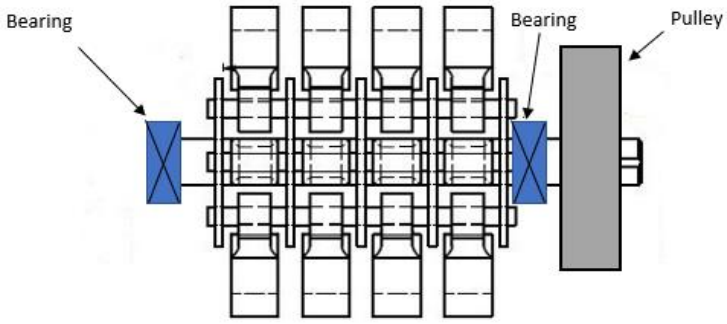

Figure 4: Rotor assembly with pulley and bearing support

In order to determine the various design parameters of the shaft, the loading of the main shaft was treated as a simply supported beam with uniformly distributed load (hammers, spacers and rods weights) which is represented as a point load acting at the center of the two bearing supports with an overhang load (pulley weight) on one side as shown in Figure 4.

Let R_1 and R_2 be the reactions at the bearing supports; F_{hsr} be the weight of the uniformly distributed load by the hammers, spacers and the mounting rod acting as a point load; F_{msp} be the combined weight of the main shaft pulley and the tight slide and slack side belt tensions.

According to Khurmi and Gupta (2010), the torsional moment on the main shaft can be obtained using Equation (12).

$$M_T = (T_{ts} - T_{ss})\, D_{msp}/2 = \frac{60P_{ms}}{2\pi N_{msp}} \qquad (12)$$

$$M_T = 2135.3 \text{ Nm}$$

where M_T is the torsional moment on the shaft due to the loading; T_{ts} *and* T_{ss} are the tight side and slack side tensions respectively.

Speed of the main shaft pulley (Vmsp) is obtained using Equation (13) (Udo et al., 2015).

$$Vmsp = (\pi \times Dmsp \times Nmsp)/60 \qquad (13)$$

$$Vmsp = 16.36 \ m/s$$

The ratio of tight side and slack side belt tension is given by Equation (14) (Udo et al., 2015).

$$\frac{T_{ts}}{T_{SS}} = 10^{\theta/(2.3 \sin \beta)} \qquad (14)$$

Substituting Equation (14) into Equation (12) and making Tss the subject gives Equation (15)

$$T_{ss} = \frac{2M_T}{D_{msp}(10^{\mu\theta/2.3 \sin \beta} - 1)} \qquad (3.15)$$

where:
β is half the groove angle of the pulley;

μ is the coefficient of friction between the belt and the pulley;

θ is the angle of lap or contact between belt and the pulley [θ=(π-2α)], and α is given by equation (16)

$$\alpha = \frac{(D_{emp} - D_{msp})}{2Ccd} \qquad (16)$$

μ=0.29

Therefore, θ = 3.01 rad

Substituting the obtained parameters into Equation (15), Tss is obtained to be

Tss = 1235.3 N

Tts was obtained to be 22587.9 N from Equation (14)

The loading, shear force diagram and the bending moment of the main shaft is represented in Figure 5. Where F_{hsr} is the loading as a result of the hammers, spacers and rods weights; and F_{msp} is the loading at the point the main shaft pulley is located on the shaft, being the summation of the tight side and slack side tension and the weight of the pulley itself. The various reactions at the bearing support were obtained.

The maximum bending moment (M_b) on the main shaft pulley was obtained to be 715.2 Nm as shown in Figure 5.

The diameter of the main shaft is determined using Equation (17) (Khurmi and Gupta, 2008).

$$D = \left[\frac{16}{\pi S_{ms}} \sqrt{(K_b M_b)^2 + (K_T M_T)^2}\right]^{1/3} \quad (17)$$

where: D is the diameter of the shaft (m); S_{ms} is the allowable shear stress of the main shaft which is 42 MN/m2; K_b and K_T are the combined shock and fatigue factors applied to bending moment and torsional moment (given as 3) due to high level of fatigue and shock; and M_b and M_T are the maximum bending and torsional moments (Nm) respectively.

D = 0.229 m 0.187 m

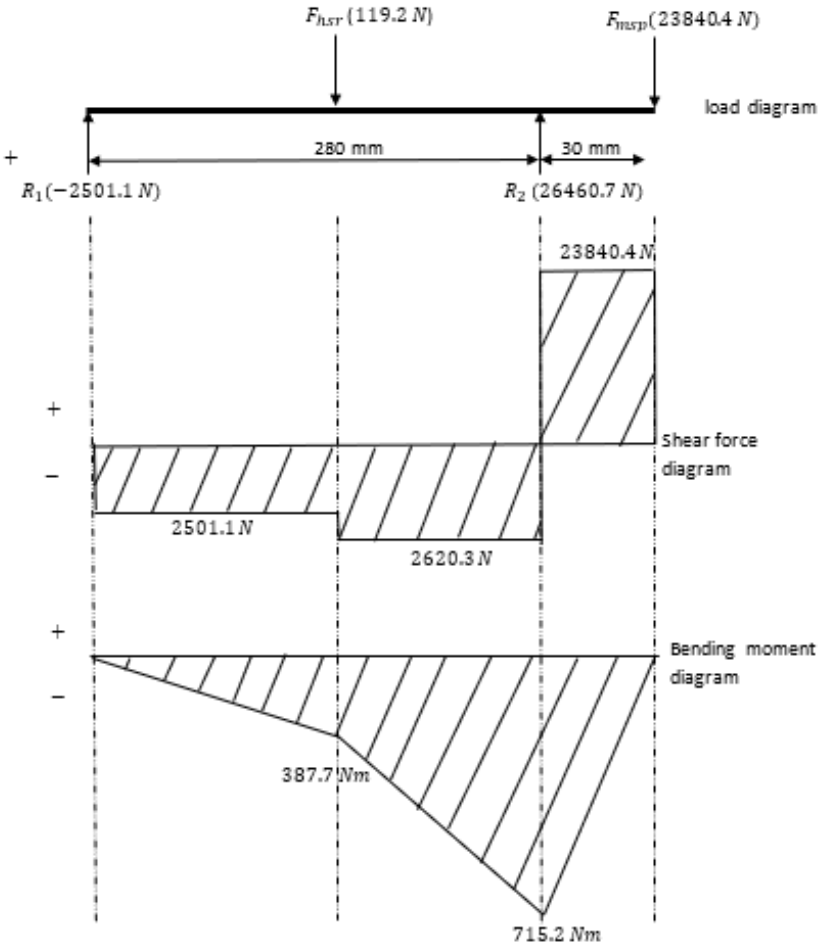

Figure 5: Load, shear force and bending moment diagram of the rotor assembly

Resolving the forces vertically, and taking moments about point R_2, R_1=-2501.1 N and R_2 = 26460.7 N

Selection of bearing

For the machine, a ball rolling contact bearing with the standard designation 307 was used. This decision was made based on the sort of load that the bearing

will carry both at rest and during operation, as well as the diameter of the shaft (Khurmi and Gupta, 2010).

Frame design

The frame assembly is shown in Figure 6 presenting different views of the machine. Design of the frame focused primarily on maximizing the frame's stiffness and strength. The frames were created from separate parts and then merged to create homogenous bodies, discounting the effect of joints on the ultimate stiffness of the frame.

FEA of the structural parts of the machine

Finite element analysis (FEA) was carried out on the 3D CAD models created in Autodesk Inventor which was used to assess the behaviour and structural stability of the rotor and frame assemblies under loading. In order to produce solid meshes for the FEA analysis, the rotor assembly and frame assembly finite element models (FEMs) were discretized into 36379 elements and 62647 nodes, respectively.

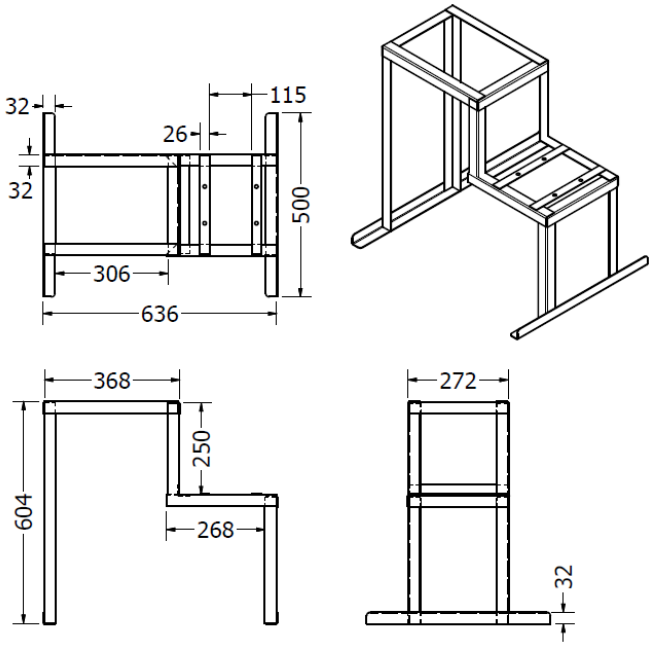

Figure 6: Frame Design

Material Selection

The material used in the fabrication of each component parts to provide an efficient, reliable, workable, stiff, and long-lasting machine is based primarily on: availability of material locally; easily rough machined or otherwise easily worked; rigidity and strength so as to be able to resist bending and to be able to carry weight of the parts; relative cheapness of the material while being able to meet the safe functional requirement.

The various component parts of the machine were fabricated using various appropriate manufacturing techniques, and assembled.

Finite Element Analysis (FEA) and Performance Evaluation

The components of the machine were analyzed using FEA in order to assess how the design works under loading conditions; and the performance evaluation of the machine.

Performance evaluation

Sun-dried Raphia seeds were fed into the machine to evaluate its performance. This was conducted by feeding a sample of 3 kg of the well sun-dried Raphia seeds into the machine and recording the output mass and time taken for the pulverization to be done. A total of five trials were conducted. The output mass was measured using a weighing balance, a stopwatch was used to monitor the time.

The following performance indicators were then determined using the average values;

i. Throughput capacity (Q_{tp})

Throughput is the rate at which the sample to passes through the machine. This was measured in kg/hr., and determined using Equation (18) given by Mohamed et al. (2015).

$$Q_{tp} = \frac{M_{out}}{T_p} \qquad (18)$$

where M_{out} is the mass of pulverized seed and Tp pulverizing time.

ii. Pulverizing efficiency (P_{eff})

It is the ratio of the mass of pulverized seed collected from the machine to the mass of seed fed into the machine. This was obtained using Equation (19) given by Oji et al. (2019).

$$P_{eff} = \frac{M_{out}}{M_{in}} x\ 100 \qquad (19)$$

where M_{in} is the mass of seed fed into the machine.

iii. Particle size distribution and analysis

The particle size distribution of crushed seed is determined using the sieving method, which involves the use of a sieve and a sieve vibrator. The sieve vibrator has 1700, 1200, 900, 600, 500, 420, and 212 µm sieve sizes arranged in decreasing sequence of size with a collector beneath them. The sieve vibrator was run for 20 minutes after 600 g of crushed seed was put into the layer of sieves. Using Equations (20) to (23), particle size analysis was performed to estimate the average particle size.

$$Ave_{ss} = \frac{USO+LSO}{2} \qquad (20)$$

$$\%M_{retained} = \frac{M_{retained}}{TM_{retained}} \times 100 \qquad (21)$$

$$M_{mean\ dia} = \frac{\sum_{i=1}^{6} P_{mean\ dia}}{\sum_{i=1}^{6} \%M_{retained}} \qquad (22)$$

$$P_{eff.bps} = \frac{M_{ts}}{M_{oversized}} \qquad (23)$$

where: Ave_{ss} is the average sieve size; *USO* and *LSO* is the upper and lower sieve openings or size; $\%M_{retained}$ percentage mass retained; $M_{retained}$ is the mass retained; $TM_{retained}$ is the total mass retained; $M_{mean\ dia}$ is the mean diameter of the mass; $P_{mean\ dia}$ particle mean diameter; $P_{eff.bps}$ is the efficiency of the machine based on the particle size analysis; M_{ts} is the total mass sieved; and $M_{oversized}$ is the mass of oversized particles.

Results and Discussion

FEA result of the rotor and frame assembly

The rotor assembly finite element (FEM) model was discretized into 36379 elements and 62647 nodes for the generation of a solid FEA mesh as shown in Figure 7.

The FEA findings revealed a maximum stress of 103.1 MN/m^2; a maximum displacement of 0.2317 mm; a maximum strain of 3.99×10^{-4} and a minimum factor of safety (FOS) of 2 with loads of 119.2 N and 3,000 N on the shaft and hammers, as presented in Figures 8 to 11 respectively. It was observed that the maximum stress on the member is less than the yield strength of (250 MN)/m^2 of the mild steel used for the parts of the rotor assembly.

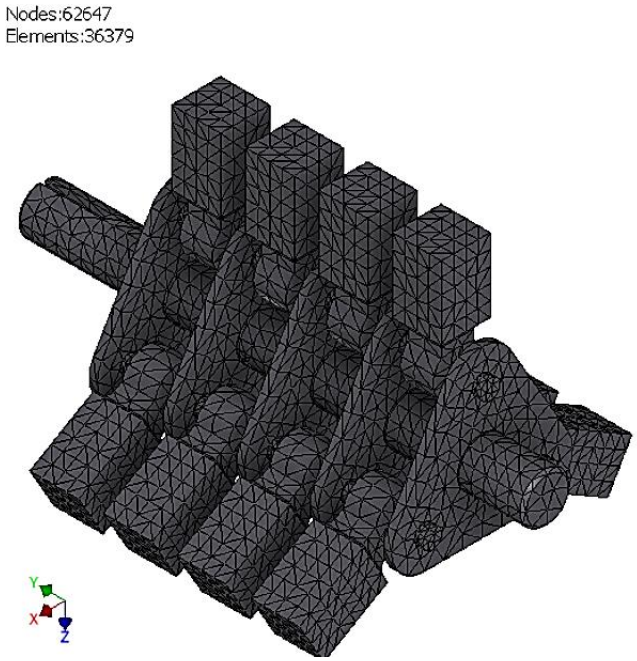

Figure 7: Rotor assembly meshing

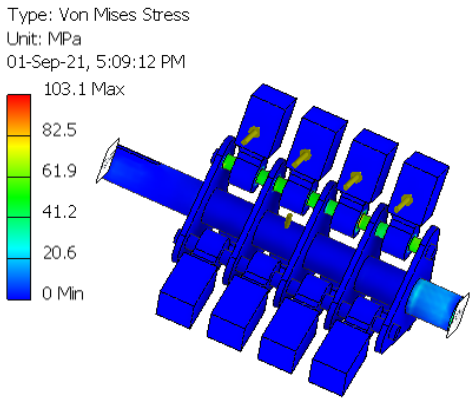

Figure 8: Stress distribution within rotor assembly members

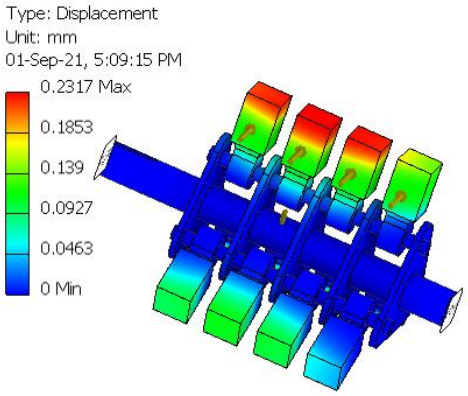

Figure 9: Resultant displacement of the rotor

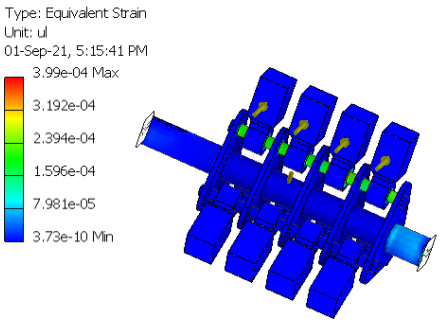

Figure 10: Equivalent strain distribution within the rotor assembly members

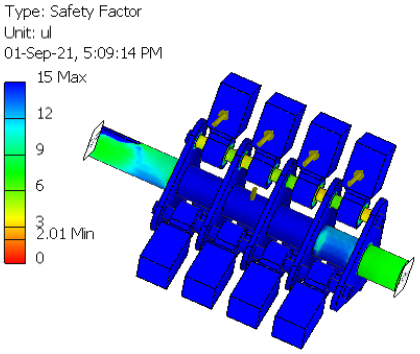

Figure 11: Factor of safety layout on the FEM of the rotor assembly

Similarly, as shown in Figures 12 to 16, the FEM model for the frame assembly was discretized into 17964 elements and 38575 nodes in order to produce its solid mesh for FEA.

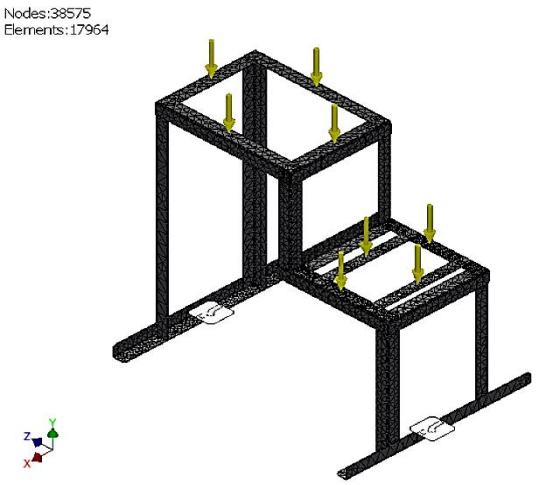

Figure 12: Frame assembly meshing

The FEA static analysis result showed that it experienced a maximum stress of 97.7 MN/m^2; a maximum resultant displacement of 0.499 mm; a maximum strain of 3.78×10^{-4} and a minimum FOS value of 2.1 when forces of 321 N and 430 N is applied representing the loading due to the weights of the entire body of the grinding unit and the electric motor, respectively, as shown in Figure 4.7 to 4.10. The maximum stress value derived from the FEA is also noted to be below the 250 MN/m^2 yield strength of mild steel used as component material.

The results of the FEA analysis implies that, under normal working conditions, both the rotor and the frame assembly will function satisfactorily as designed without failing under loading, as the maximum stress values obtained from the FEA of their components are well below the respective point of yielding of selected materials.

Productivity and efficiency test

The result of the test carried out by feeding a sample of 3kg of Raphia seed in the machine for pulverization is presented on Table 1.

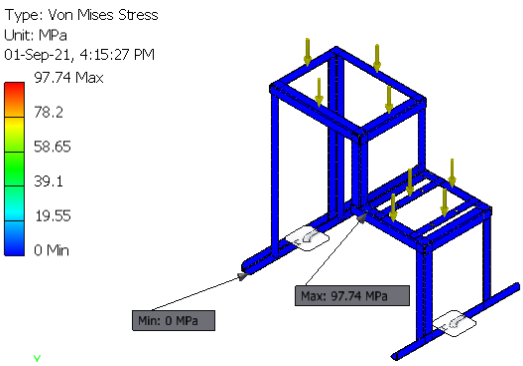

Figure 13: Stress distribution within frame assembly members

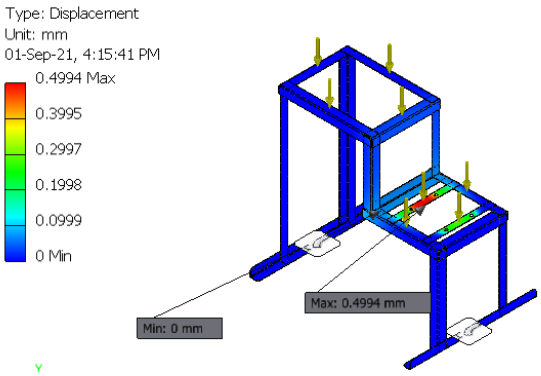

Figure 14: Resultant displacement of the frame assembly members

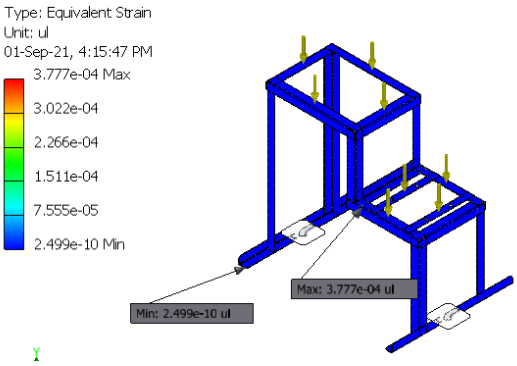

Figure 15: Equivalent strain distribution within the frame assembly members

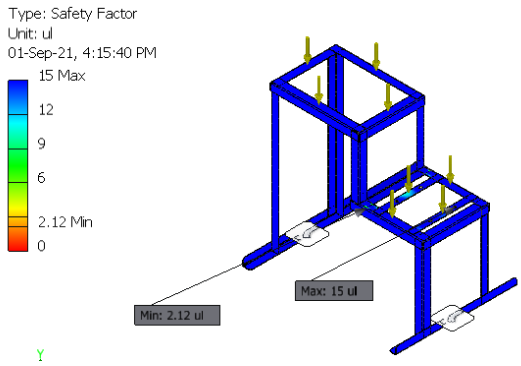

Figure 16: Factor of safety layout on the FEM of the frame assembly

Table 1: Performance evaluation test result

Test sample	Mass before pulverizing (kg)	Mass after pulverizing (kg)	Time (secs)
1	3.00	2.91	930
2	3.00	2.90	900
3	3.00	2.93	894
4	3.00	2.89	810
5	3.00	2.90	886
Average	**3.00**	**2.91**	**884**

Throughput (Q_{tp}) is 11.85 kg/hr;and Pulverizing Efficiency (P_{eff}) is 97%

A throughput and pulverizing efficiency of 11.85kg/h and 97% were obtained respectively, and this implies that there was 3% mass loss during the testing. Aside the effectiveness of the hammers in crushing the seeds, the high pulverizing efficiency obtained is also because the particles of the seed were not sticking to the wall of milling chamber and other moving parts.

Particle size distribution

The result of the particle size distribution experiment that was carried out using 600g of the pulverized Raphia seed is presented in Table 2.

It can be seen that the overall mass retained was 599.6 g, which is some fraction less than the mass of the sample used for the experiment. This is owing to the fact that some of the particles must have been lost due to the equipment's vibration. Also, at the 1700 and 1200 µm sieve sizes, 8.1 g and 11.88 g of the Raphia seed particle were retained, respectively. Because the machine screen is designed to be 1000 µm, these particles are considered over-sized.

The average particle size was then determined by particle size analysis, and the results are shown in Table 3.

The average particle size of 624 µm was obtained.

The pulverizing efficiency based on the particle size analysis was obtained considering the mass retained in sieve sizes 1200 and 1700 µm as oversized. (the screen designed for the machine is 1000 µm). A pulverizing efficiency of 96.82% was obtained.

From Table 3, it can be seen that at (212, 420, 500, 600, 900, 1200, and 1700) µm screens, 4.4%, 8.0%, 4.1%, 33.7%, 46.4%, 2.0%, and 1.4% of the particle sizes were retained respectively. The sieve sizes, 900µm and 600µm, both retained a much higher percentage of the material. As a result, the average particle size (624µm) found falls between 600 and 900µm. This result is in agreement with the design. This implies that the machine can effectively pulverize the seed to an average particle size of 624 µm when a 1000 µm screen is used in the milling chamber, as indicated by the 96.82% efficiency attained based on particle size distribution. Figures 17 shows the Orthographic and Isometric drawings, while Figure 18 show the exploded drawing of the machine.

Table 2: Particle size distribution

S/N	Sieve Size (µm)	Mass Retained (g)
1	1700	8.1
2	1200	11.88
3	900	269.28
4	600	195.45
5	500	24.07
6	420	46.4
7	212	25.5
8	Pan	19.10
Total		**599.6**

Table 3: Particle size analysis of the pulverized Raphia seed

Sieve Size (µm)	Average Sieve Size (µm)	$M_{retained}$ (g)	$\%M_{retained}$ (%)	$P_{mean\ dia}$ (µm)
212	106	25.50	4.4	465.5
420	316	46.40	8.0	2525.0
500	460	24.07	4.1	1906.8
600	550	195.45	33.7	18512.3
900	750	269.28	46.4	34779.9
1200	1050	11.88	2.0	2148.2
1700	1450	8.10	1.4	2022.6
Total		**580.68**	**100**	**62360.4**

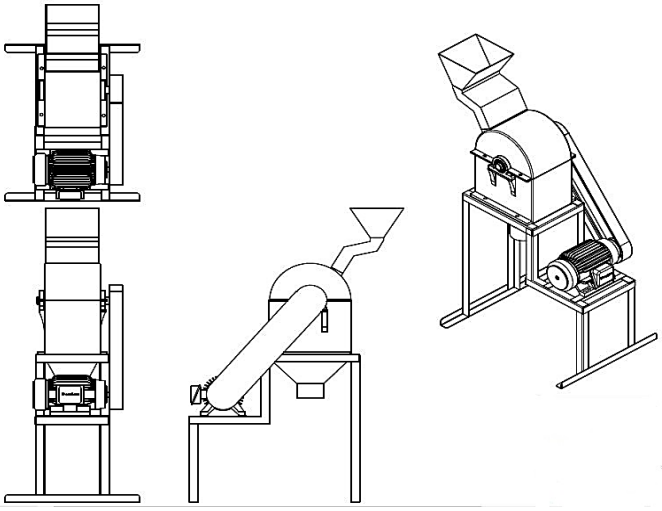

Figure 17: Orthographic and Isometric drawing of the machine

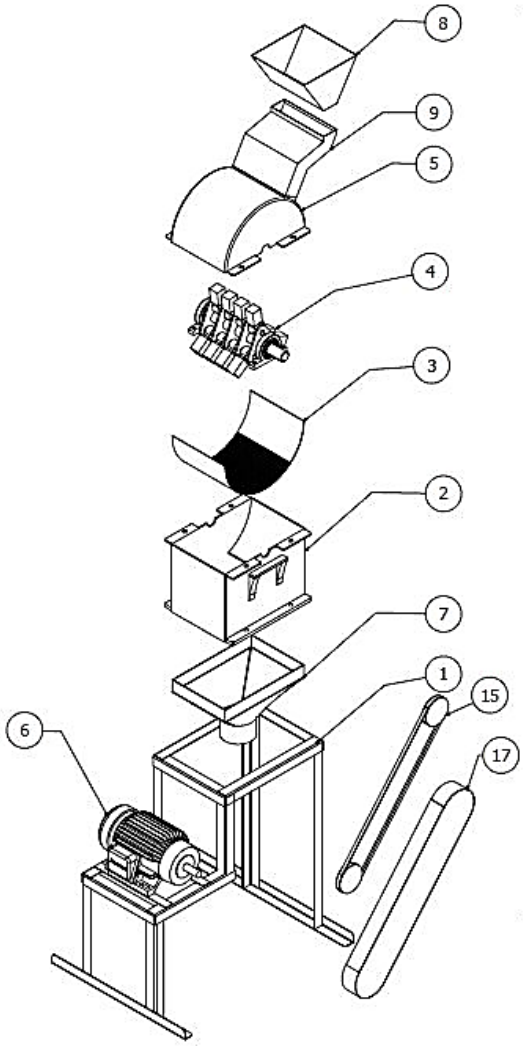

PARTS LIST		
ITEM	QTY	PART NUMBER
1	1	Frame
2	1	Lower casing
3	1	Screen
4	1	Rotor assembly
5	1	Upper casing
6	1	Electric motor
7	1	Buttom plate
8	1	Hopper
9	1	Delivery duct
10	1	ANSI/AFBMA 16.1 - 30 x 62 x 18
11	1	Bearing 80706 GOST 9592-75
12	1	Clamp KV-30 GOST 17678-80
13	1	V-Belt
14	1	Grooved Pulley1
15	1	Grooved Pulley2
16	2	bearing holder
17	1	belt cover

Figure 18: Exploded view of the Raphia seed pulverizing machine

Conclusion

A pulverizing machine for Raphia seeds was developed and evaluated. The FEA static analysis result showed that it experienced a maximum stress of 97.7 MN/m^2; a maximum resultant displacement of 0.499 mm; and a maximum strain of 3.78×10^{-4} when forces of 321 N and 430 N were applied, representing the loading due to the weights of the entire body of the grinding unit and the electric motor, and is not susceptible to structural failure during operation. Performance evaluation revealed the machine has a throughput of 11.85 kg/hr., a pulverizing efficiency of 97% and can pulverize to an average particle size of 624 µm.

References

Akpan, E. J. and Usoh, I. F. (2004): Phytochemical screening and effect of aqueous root extract of Raphia hookeri (raffia palm) on metabolic clearance rate of ethanol in rabbits. Biokemistri, 16(1): 37-42.

Atadashi, M., Aroua, M., Abdul, R. and Abdul, A. (2013): The Effects of Catalysts in Biodiesel Production: A Review. Journal of Industrial and Engineering Chemistry. 19, 14 – 26. 10.1016/j.jiec.2012.07.009.

BP (2017): BP Energy Outlook, Energy Outlook, 1–103.

Dauda, S. M., Ismail, F., Balami, A. A, Aliyu, M., Mohammed, I. S. and Ahmad, D. (2018): Physical and mechanical properties of raphia palm kernel at different moisture contents. Food Research 3(4):305-312.

Egbe, E. A. P. and Olugboji, O. A. (2016): Design, fabrication and testing of a double roll crusher. International Journal of Engineering Trends and Technology (IJETT), 35(11):511-515.

EIA (2016): International Energy Outlook 2016 with Projections to 2040, U S Energy Information Administration, 2016, DOE/EIA-0484, p. 1–290.

Fabunmi, O. A. Omeiza U. and Alabadan B. A. (2015): Physical and mechanical properties of Raphia (raphia farinifera) seed essential for handling and processing operations. International Engineering Conference, www.seetconf.futminna.edu.ng. p. 61-70.

Fapetu, O. P., Akinola, A. O., Lajide L. L. and Osasona, A. B. (2018): Physicochemical characteristics study of oil extracted from raffia palm seed. FUTA Journal of Engineering and Engineering Technology, 12(1): 102-114.

Garg, S. K., Garg, R. and Garg, R. (2007): Environmental Science and Ecological Studies. Second revised edition, Khanna Publishers, New Delhi India.

Kawuyo, U. A., Lawal, A. A., Abdulkadir J. A. and Dauda Z. A. (2017): Performance evaluation of a developed grain milling machine. Arid Zone Journal of Engineering, Technology and Environment, 13(1): 1-5.

Khurmi, R. S., and Gupta, J. K. (2010): A Textbook of Machine Design. Ram Nagar, New Delhi: Eurasia publishing house (PVT.).

Kovács, A. and Kerényi G. (2019) Physical characteristics and mechanical behaviour of maize stalks for machine development. International Agrophysics, 33(4): 427-436.

Lund, H. and Salgi, G. (2009): The role of compressed air energy storage (CAES) in future sustainable energy systems, Energy Conversion and Management, 50, 1172–1179.

Mohammed, T. H., Radwan, H. A., Elashhab, A. H., and Adly, M. Y. (2015). Design and Evaluate of a Small Hammer Mill. Egypt Journal of Agricultural Research. 93(5)(B). 481-495

Ngabea, S. A, Okonkwo, W. I. and Liberty, J. T. (2015): Design, fabrication and performance evaluation of a magnetic sieve grinding machine. Global Journal of Engineering Science and Researches, 2(8): 65-72.

Oji, N., Gwarzo, M., Mohammed, U., Abubakar, I., John, A., Zakariyah, A. and Adamu, E. (2019). Design and Construction of a Small-Scale Sugarcane Juice Extractor. Asian Research Journal of Agriculture. 1-8.

Oshewolo, S. (2012). Designed to Fail? Nigerilas Quest for Biodiesel. Asian Journal of Social Science. 3. 1 - 16

Owusu P. A. and Asumadu-Sarkodie S. (2016): A review of renewable energy sources, sustainability issues and climate change mitigation, Cogent Engineering, 3(1), 1167990.

Ramages, J. and Scurlock, J. (1996): Biomass in Renewable Energy Power for a Sustainable Future; Boyle, G., Ed.; Oxford University Press: Oxford, UK.

Shan, Y., Liao, Q., Yuan, J., Wan, X. and Lian, y. (2024): Effects of Cutting Parameters on the Shearing Properties of Oilseed Rape (Brassica Napus L.) Shoots in Harvesting. Applied Engineering in Agriculture. 40(3): 339 - 349

Udo, S., Adisa, F., Ismaila, O. and Adejuyigbe, S.B. (2015). Development of palm kernel nut cracking machine for rural use. Agricultural Engineering International: CIGR Journal. 17. 397-406.

Ugwuegbu, C. C., Ogbonna, A. I., Ikele, U. S., Anaele, J. U., Ochieze, U. P. and Onwuegbuchulam, A. (2017): Design, construction and performance analysis of a 5 kg laboratory ball mill. Global Journal of Researches in Engineering: A Mechanical and Mechanics Engineering, 17(2):27-42